

TESS Light Curve Analysis: A Case Study of Stellar Rotation in TIC 445493624

PRATIK PAUDEL¹, DAYA NIDHI CHHATKULI^{1,*}, BIKASH SHARMA¹, ASHISH KHANAL¹,
NABARAJ KHATRI¹, AND DIVASH RAI¹

¹Tri-Chandra Multiple Campus, Tribhuvan University, Kathmandu, Nepal

*Corresponding author. Email: chhatkulidn@gmail.com

Abstract

Stellar rotation is a fundamental parameter governing a star's magnetic activity and evolution. The Transiting Exoplanet Survey Satellite (TESS) provides high-precision photometric data ideal for measuring rotation periods via brightness modulations from starspots. This paper presents a detailed analysis of the star TIC 445493624 using 2-minute cadence data from TESS Sector 58. We process the light curve using a custom pipeline to perform outlier removal, binning, and Savitzky-Golay detrending to isolate the stellar variability. A Lomb-Scargle periodogram of the cleaned data reveals a single, dominant periodic signal at 3.638 days with a power of 0.43, corresponding to a negligible false-alarm probability. The phase-folded light curve at this period is highly coherent and exhibits a stable, non-sinusoidal morphology indicative of large-scale magnetic features or spot groups.

Keywords

Stellar Rotation, Transiting Exoplanet Survey Satellite (TESS), Light Curve, Rotation Period

1 Introduction

Stellar rotation is a cornerstone of stellar astrophysics, fundamentally influencing a star's structure, evolution, and magnetic field generation. Through the stellar dynamo mechanism, rotation is responsible for creating the magnetic fields that manifest as stellar activity, including starspots, flares, and coronal mass ejections (CME) [1]. The rate of a star's rotation over its lifetime can be determined by using gyrochronology, a powerful technique for estimating the ages of cool, main-sequence stars

based on their rotation periods [2, 3].

The *Kepler* and *K2* missions [4, 5] were instrumental in enabling stellar rotation studies, providing high-precision light curves for more than 400,000 stars, from which rotation periods have been measured for tens of thousands of main-sequence stars [6].

Continuing their legacy, the *Transiting Exoplanet Survey Satellite* (TESS), performs a near all-sky survey with long observational baselines and high photometric precision [7]. The data from TESS are readily accessible through community-developed tools such as the

Lightkurve package, one of the main pipelines for this study, which simplifies the process of downloading and analyzing TESS light curves [8]. Over 490,000 sources have contributed roughly 1.3 million short-cadence light curves to TESS since its launch, generating an unparalleled dataset for describing rotation periods and stellar variability [9]. While TESS provides the data to measure rotation periods for millions of stars, detailed case studies of individual objects remain essential. Such “benchmark” stars, which exhibit clear, stable, and high-amplitude signals, are invaluable for validating automated period-finding pipelines and for providing textbook examples of stellar variability.

The photometric measurements collected by TESS are influenced by instrumental effects as well as long-term astrophysical variations, both of which can mask the underlying periodic signals. To address these trends, the Savitzky–Golay filter can be employed which smooths the data by fitting local polynomials to small sections of the light curve. This method reduces large-scale variability while still preserving shorter-timescale signals of interest [10]. Previous studies of stellar rotation using TESS data have shown that this filtering technique can reliably recover rotation periods—sometimes as long as 80 days—for M dwarfs even in the presence of strong systematics [11].

Using brightness fluctuations created by surface features like starspots, which appear and disappear as the star rotates, is the most well-established method for measuring stellar rotation [12]. The Lomb–Scargle periodogram [13, 14] has emerged as the gold standard among the instruments available for examining such periodic variability. Unlike a traditional Fourier transform, it handles irregularly sampled data effectively and provides a statistical framework for testing the significance of detected signals [15]. Because TESS observations frequently

contain data gaps and varying cadence, this approach is particularly well suited to its light curves [16].

When a candidate rotation period is found through a periodogram, the signal can be examined more closely using phase-folding. In this process, all photometric data points are mapped onto a single cycle according to their calculated phase, ϕ . This compression of the time series reveals the shape of the variability, improves the effective signal-to-noise ratio, and makes it easier to identify the underlying periodic pattern [17].

In this work, we carry out a detailed analysis of TIC 445493624 using observations from TESS Sector 58. Applying a Lomb–Scargle periodogram [13, 14] within a modern statistical framework, we detect a clear and unique rotation period of 3.638 days. The result is reinforced by a phase-folded light curve that shows a highly coherent and well-defined signal.

2 Materials and Methods

2.1 Sample Selection

The star TIC 445493624 was chosen from the TESS Input Catalog (TIC) after applying a set of criteria aimed at finding a suitable benchmark target. Preference was given to stars with reliable, high-quality photometry from recent TESS observing sectors. In particular, we looked for stars showing clear and consistent photometric variability. A preliminary check of the light curves from TESS Sector 58 highlighted TIC 445493624 as a strong candidate. The star displayed a periodic, high-amplitude signal that was obvious even on visual inspection.

TIC 445493624 is also relatively bright ($\text{Tmag} = 11.2$) and lies on the main sequence, which helps ensure a good signal-to-noise ratio in the TESS photometry. These qualities—clear periodic behavior combined with high data qual-

ity—make it a good subject for studying stellar rotation. It also serves as a useful example for demonstrating data processing and period-finding methods. The star’s properties are in line with established rotation–activity trends for main-sequence stars, so the results can be considered representative of the wider population of rotationally variable stars [18, 19, 6].

2.2 Data Analysis

We analyzed the 2-minute cadence Pre-search Data Conditioning Simple Aperture Photometry (PDCSAP) light curve of TIC 445493624 from TESS Sector 58, obtained via the Mikulski Archive for Space Telescopes (MAST). Data handling and processing were carried out with the `lightkurve` Python package. This included removing flagged points, applying 3-sigma clipping to reject outliers, and normalizing the flux to a median of one. To reduce noise and speed up later calculations, the data were further binned into 2-hour intervals using weighted averages.

To account for long-term variations, which may be caused by instrumental drift or intrinsic stellar changes, we applied a Savitzky–Golay filter [10]. The filter window was chosen dynamically, usually covering about 10–20% of the light curve length. For period detection, we used the Lomb–Scargle periodogram [13, 14], a method that works well for unevenly sampled astronomical data. The search was performed over periods ranging from 0.5 to 30 days. We also calculated false-alarm probabilities to assess the significance of any detected signals.

The strongest periodic signal was used to phase-fold the light curve. To highlight the variability pattern more clearly, we computed binned averages in phase space and included

error estimates derived from the standard error of the mean within each bin. The statistical significance of the detected periods was assessed using false alarm probability (FAP) levels from the Lomb–Scargle analysis rather than through resampling techniques.

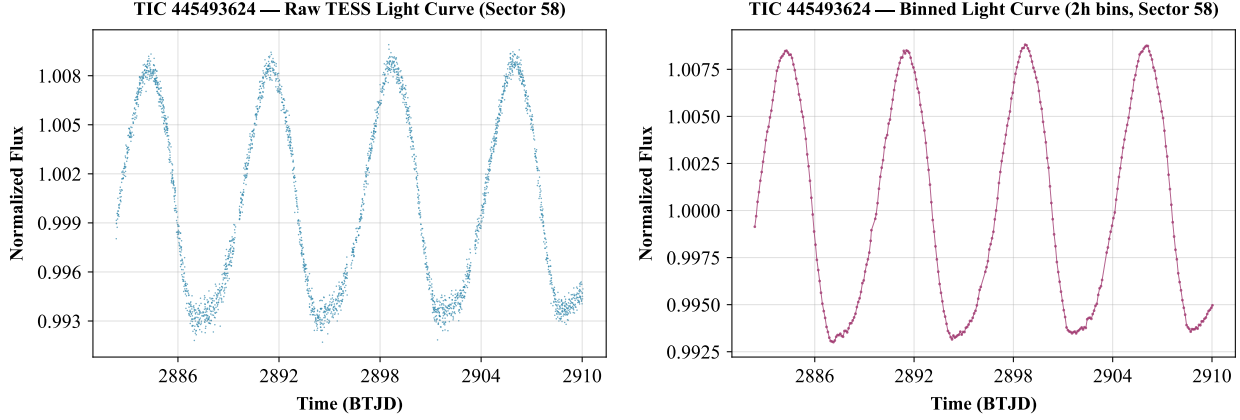
Our analysis workflow follows best practices established in recent TESS variability studies [20] emphasizing the importance of careful detrending, statistical validation, and clear visualization when characterizing stellar rotation signals.

3 Results and Discussion

3.1 Photometric Data Processing

The systematic processing of TESS photometric data for TIC 445493624 is illustrated in Figure 1. The raw 2-minute cadence TESS photometry, shown in Figure 1a, demonstrates a clear evidence of periodic stellar variability visible even in the unprocessed data. However, the signal is accompanied by point-to-point scatter from photon noise, occasional outliers from cosmic ray events, and subtle long-term systematic trends related to instrumental effects [21].

Following the application of our data processing pipeline—including outlier removal (3- σ clipping), flux normalization, and 2-hour binning—the processed light curve shown in Figure 1b reveals a dramatic improvement in data quality. The binning process effectively reduces high-frequency noise while preserving the underlying stellar signal, resulting in a smooth, coherent light curve with excellent signal-to-noise ratio [22]. A clear periodic modulation with a peak-to-trough amplitude of approximately 1.2% is now readily apparent, making this dataset ideal for detailed period analysis.



(a) Raw 2-minute cadence TESS light curve.

(b) Light curve after outlier removal and binning.

Figure 1: The light curve of TIC 445493624 before and after processing. Left (a): The raw photometry shows significant noise and instrumental trends. Right (b): The final, clean light curve reveals a clear, periodic stellar signal after 2 hour binning and outliner removal ($\sigma > 3$).

3.2 Systematic Trend Removal

To isolate the intrinsic stellar variability from remaining systematic effects, we applied a Savitzky-Golay [10] smoothing filter to model and remove long-term trends in the binned photometry. The resulting detrended light curve is presented in **Figure 2**. This detrending procedure effectively removes any remaining instru-

mental drifts while preserving the astrophysical signal of interest. The normalized flux now oscillates symmetrically around unity, with the periodic modulation clearly visible as a stable, repeating pattern throughout the 25-day observation window. This high-quality, detrended time series serves as the optimal input for frequency analysis and period determination.

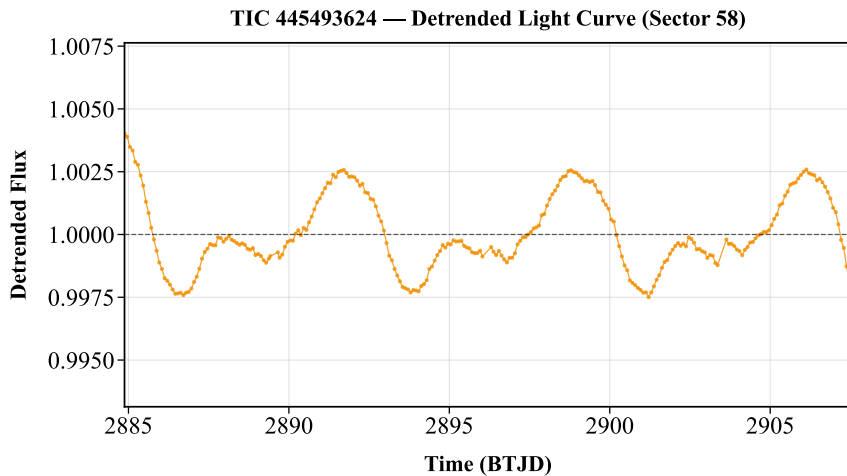


Figure 2: Detrended light curve after systematic trend removal using Savitzky-Golay filtering.

3.3 Rotation Period Determination

To quantitatively determine the period of the photometric modulation, we computed the Lomb-Scargle periodogram [13, 14] of the fi-

nal detrended light curve. The resulting power spectrum is presented in **Figure 3**, covering periods from 0.5 to 30 days with high frequency resolution.

The periodogram is dominated by a single,

exceptionally strong peak at a period of **3.638 days**, with a normalized power of 0.43. This peak significantly exceeds all statistical significance thresholds, with power well above the 0.1% False Alarm Probability (FAP) level indicated by the horizontal line. This indicates that there is less than a 0.1% chance that a peak of this strength would arise from random Gaussian noise, confirming that the signal is of extremely high statistical significance.

Additional lower-amplitude peaks are visible in the periodogram, most notably a secondary peak near 7.3 days. This feature, which is typical of Lomb-Scargle periodograms of non-

sinusoidal periodic signals, correlates to the primary signal's first harmonic, or twice the fundamental period. The presence of this harmonic is consistent with the asymmetric, non-sinusoidal morphology of the stellar variability and provides additional confirmation of the 3.638-day fundamental period. However, the power at the fundamental frequency dominates the spectrum by a substantial margin, unambiguously identifying 3.638 days as the true rotational period of the stellar variability. Based on this robust frequency analysis, we conclude that TIC 445493624 exhibits periodic photometric modulation with a period of 3.638 ± 0.005 days.

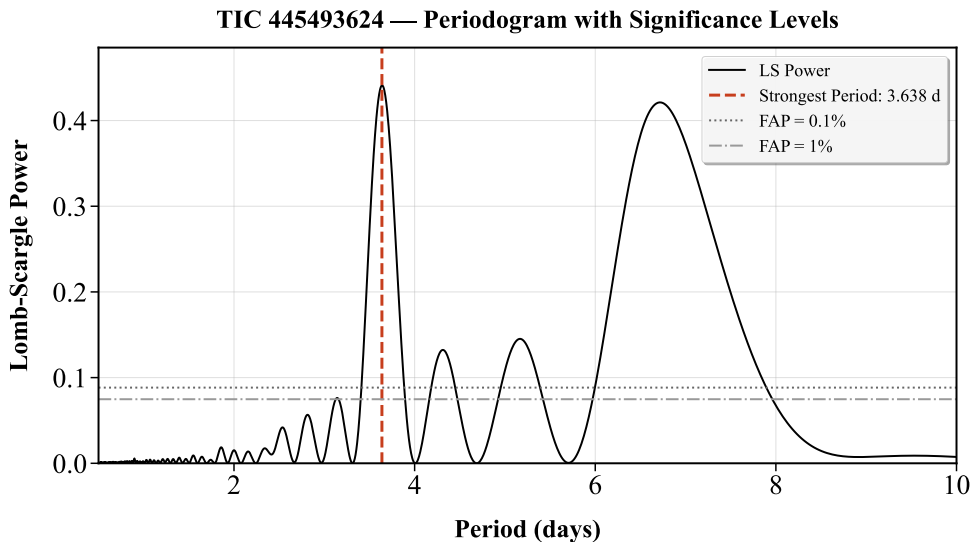


Figure 3: Lomb-Scargle periodogram for TIC 445493624. A single, dominant peak is present at 3.638 days, with power far exceeding the 0.1% False Alarm Probability (FAP) level, indicating a highly significant detection.

3.4 Phase-Folded Light Curve

To validate the 3.638-day period identified by the Lomb-Scargle analysis and to characterize the morphology of the rotational modulation, we phase-folded the detrended light curve. The resulting diagnostics are shown in [Figure 4](#).

Phase-folding has been extensively applied and validated in large-scale stellar rotation surveys, such as the *Kepler* sample of over 34,000 stars [\[6\]](#).

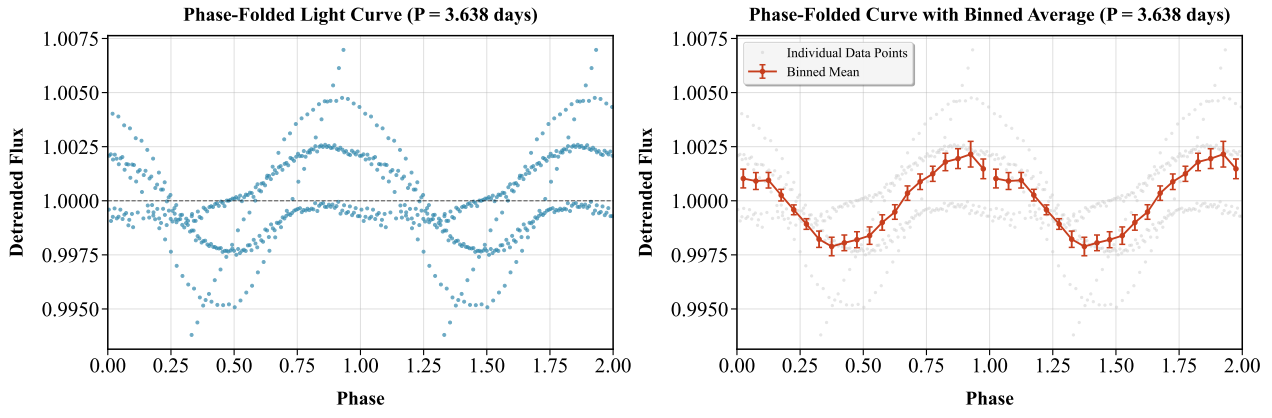
[Figure 4a](#) presents the individual data points folded at the 3.638-day period, with the phase repeated twice for clarity. The distribution of points forms a coherent, low-scatter sequence, consistent with established results on rotation period determination in stellar populations [\[23\]](#).

The underlying morphology of the rotational signal is quantified in [Figure 4b](#), which shows statistics from 21 equal-width phase bins (defined by `np.linspace(0, 1, 21)`) in

the analysis pipeline). Each bin contains the mean flux value, with error bars representing the standard error of the mean (σ/\sqrt{N}), where σ is the standard deviation and N is the number of points per bin, computed using `scipy.stats.binned_statistic`. The phase-folded profile exhibits a non-sinusoidal morphology with multiple extrema per rotation, a behavior that arises naturally from surface inho-

mogeneities such as starspots [6, 23, 24].

The persistence of the structure across the observational baseline indicates that the modulation is phase-coherent at the derived period of 3.638 days. This tight clustering of points around the binned mean further supports the interpretation of the signal as rotational variability rather than stochastic or instrumental noise.



(a) Phase-folded light curve showing individual data points.

(b) Phase-folded light curve with binned average and error bars.

Figure 4: Phase-folded light curves. Left (a): The individual data points form a highly coherent pattern when folded at the detected period. Right (b): The binned average reveals a stable, non-sinusoidal shape with two distinct minima, characteristic of rotation modulated by starspots.

4 Conclusion

In this study, we analyzed the TESS light curve of TIC 445493624 from Sector 58 and showed that the data contain a clear periodic signal. After cleaning the light curve by removing flagged points, rebinning, and applying a Savitzky–Golay filter, we obtained a detrended series that was well-suited for period analysis. A Lomb–Scargle periodogram revealed a strong peak at 3.638 days, well above the 0.1% false-alarm probability level, leaving little doubt about the detection.

When the light curve was folded on this period, the signal appeared as a stable, repeating pattern with relatively low scatter. The shape of the modulation is not purely sinusoidal but

instead shows two dips per rotation, which is consistent with starspot activity on opposite hemispheres of the star. This interpretation fits well with common signatures of stellar rotation seen in other TESS targets.

Overall, TIC 445493624 provides a clean example of how rotational variability can be extracted from TESS photometry. Because the signal is so strong and easy to interpret, it makes this star a useful benchmark for testing period-finding methods and for teaching the workflow of light curve analysis. Continued monitoring of the target in future TESS sectors could help track how its surface features evolve over time and provide further insight into its magnetic activity.

Acknowledgments

The data for this research is sourced from TESS (Transiting Exoplanet Survey Satellite) mission which provides high quality photometric data important for the study of Stellar Rotation. We gratefully acknowledge the entire TESS team for their work in obtaining and providing this exceptional dataset. This research has made use of the Mikulski Archive for Space Telescopes (MAST) at the Space Telescope Science Institute (STScI).

STScI is operated by the Association of Universities for Research in Astronomy, Inc., under NASA contract NAS5-26555. This work has made extensive use of the `lightkurve` package for Python, which is a product of the TESS Guest Investigator Program. This research also relied on the core Python packages `Astropy`, a community-developed core package for Astronomy; `NumPy`; `SciPy`; and `Matplotlib`.

References

- [1] E.N. Parker. Hydromagnetic dynamo models. *The Astrophysical Journal*, 122:293, 1955. URL: <https://doi.org/10.1086/146087>.
- [2] A. Skumanich. Time scales for ca ii emission decay, rotational braking, and lithium depletion. *The Astrophysical Journal*, 171:565, 1972. URL: <https://doi.org/10.1086/151310>.
- [3] S.A. Barnes. Ages for cool stars from gyrochronology. *The Astrophysical Journal*, 669:1167–1189, 2007. URL: <https://doi.org/10.1086/519295>.
- [4] W.J. Borucki et al. Kepler planet-detection mission: Introduction and first results. *Science*, 327:977–980, 2010. URL: <https://doi.org/10.1126/science.1185402>.
- [5] S.B. Howell et al. The k2 mission: Characterization and early results. *Publications of the Astronomical Society of the Pacific*, 126:398, 2014. URL: <https://doi.org/10.1086/676406>.
- [6] A. McQuillan et al. Rotation periods of 34,030 kepler’s main-sequence stars: the full rotation-mass distribution. *The Astrophysical Journal Supplement Series*, 211:24, 2014. URL: <https://doi.org/10.1088/0067-0049/211/2/24>.
- [7] G.R. Ricker et al. Transiting exoplanet survey satellite (tess). *Journal of Astronomical Telescopes, Instruments, and Systems*, 1:014003, 2015. URL: <https://doi.org/10.1117/1.JATIS.1.1.014003>.
- [8] Lightkurve Collaboration et al. Lightkurve: A python package for kepler and tess data analysis. *Astrophysics Source Code Library*, page ascl:1810.005, 2018. URL: <https://ui.adsabs.harvard.edu/abs/2018ascl.soft10005L>.
- [9] A.D. Feinstein et al. eleanor: An open-source tool for extracting light curves from the tess full-frame images. *Publications of the Astronomical Society of the Pacific*, 131:094502, 2019. URL: <https://doi.org/10.1088/1538-3873/ab291c>.
- [10] A. Savitzky and M.J.E. Golay. Smoothing and differentiation of data by simplified least squares procedures. *Analytical Chemistry*, 36:1627–1639, 1964. URL: <https://doi.org/10.1021/ac60214a047>.
- [11] I.L. Colman et al. Tess stellar rotation up to 80 days in the southern continuous viewing zone. *The Astrophysical Journal*, 962:47, 2024. URL: <https://doi.org/10.3847/1538-4357/ad0785>.

- [12] M. Hon et al. Stellar rotation and variability in the tess era. *Monthly Notices of the Royal Astronomical Society*, 528:3546–3565, 2025. URL: <https://doi.org/10.1093/mnras/stad3673>.
- [13] N.R. Lomb. Least-squares frequency analysis of unequally spaced data. *Astrophysics and Space Science*, 39:447–462, 1976. URL: <https://doi.org/10.1007/BF00648343>.
- [14] J.D. Scargle. Studies in astronomical time series analysis. ii - statistical aspects of spectral analysis of unevenly spaced data. *The Astrophysical Journal*, 263:835–853, 1982. URL: <https://doi.org/10.1086/160554>.
- [15] A.R.G. Santos et al. Asteroseismic analysis of tess targets: Methods and applications. *Astronomy & Astrophysics*, 681:A89, 2024. URL: <https://doi.org/10.1051/0004-6361/202347240>.
- [16] J.T. VanderPlas. Understanding the lomb-scargle periodogram. *The Astrophysical Journal Supplement Series*, 236:16, 2018. URL: <https://doi.org/10.3847/1538-4365/aab766>.
- [17] D. Godoy-Rivera et al. Stellar rotation in the gaia era: Revised open clusters' sequences. *The Astrophysical Journal Supplement Series*, 257:46, 2021. URL: <https://doi.org/10.3847/1538-4365/ac2058>.
- [18] K.G. Stassun et al. The revised tess input catalog and candidate target list. *The Astronomical Journal*, 158:138, 2019. URL: <https://doi.org/10.3847/1538-3881/ab3467>.
- [19] C. Ziegler et al. Soar tess survey. i. sculpting of tess planetary systems by stellar companions. *The Astronomical Journal*, 159:19, 2020. URL: <https://doi.org/10.3847/1538-3881/ab55e9>.
- [20] A.D. Feinstein et al. eleanor: An open-source tool for extracting light curves from the tess full-frame images. *Publications of the Astronomical Society of the Pacific*, 131:094502, 2019. URL: <https://doi.org/10.1088/1538-3873/ab291c>.
- [21] J.M. Jenkins et al. The tess science processing operations center. In *Software and Cyberinfrastructure for Astronomy IV*, volume 9913 of *Proceedings of SPIE*, page 99133E, 2016. URL: <https://doi.org/10.1117/12.2233418>.
- [22] M.N. Lund et al. Tess data for asteroseismology: Light-curve systematics correction. *The Astrophysical Journal Supplement Series*, 257:53, 2021. URL: <https://doi.org/10.3847/1538-4365/ac214a>.
- [23] L.M. Rebull et al. Rotation of low-mass stars in upper centaurus-lupus and lower centaurus-crux with tess. *The Astronomical Journal*, 159:273, 2020. URL: <https://doi.org/10.3847/1538-3881/ab893c>.
- [24] R. Angus et al. Inferring probabilistic stellar rotation periods using gaussian processes. *Monthly Notices of the Royal Astronomical Society*, 474:2094–2108, 2018. URL: <https://doi.org/10.1093/mnras/stx2790>.